

Resonant Mode Coupling in δ Scuti Stars

MOHAMMED MOURABIT¹ AND NEVIN N. WEINBERG¹

¹*Department of Physics, University of Texas at Arlington, Arlington, TX 76019, USA*

ABSTRACT

Delta Scuti (δ Sct) variables are intermediate mass stars that lie at the intersection of the main sequence and the instability strip on the Hertzsprung-Russel diagram. Various lines of evidence indicate that nonlinear mode interactions shape their oscillation spectra, including the particularly compelling detection of resonantly interacting mode triplets in the δ Sct star KIC 8054146. Motivated by these observations, we use the theory of three-mode coupling to study the strength and prevalence of nonlinear mode interactions in fourteen δ Sct models that span the instability strip. For each model, we calculate the frequency detunings and nonlinear coupling strengths of $\sim 10^4$ unique combinations of mode triplets. We find that all the models contain at least ~ 100 well-coupled triplets whose detunings and coupling strengths are consistent with the triplets identified in KIC 8054146. Our results suggest that resonant mode interactions can be significant in δ Sct stars and may explain why many exhibit rapid changes in amplitude and oscillation period.

1. Introduction

The δ Sct stars are pulsating variables that are on, or slightly past, the main sequence and have masses between 1.5 and $2.5M_{\odot}$, effective temperatures between 6400 and 8600 K, and stellar types between A and F (for reviews, see Breger 2000; Goupil et al. 2005; Catelan & Smith 2015; Guzik 2021; Aerts 2021). Their oscillations are driven by the opacity (κ -) mechanism in the second partial ionization zone of helium and consist of low order p - and g -modes with oscillation periods ranging from 15 min to 8 hour (frequencies from a few to 100 cycles per day). The photometric amplitudes are often a few milli-magnitudes but can exceed a tenth of a magnitude in high amplitude δ Sct stars (HADS).

The oscillation spectra from the four-year light curves of the *Kepler* space mission provided unprecedented frequency resolution for over a thousand δ Sct stars (see, e.g., Balona & Dziembowski 2011; Uytterhoeven et al. 2011; Bowman & Kurtz 2018). By surveying the entire sky, the *TESS* space mission has delivered month-long light curves for over ten thousand δ Sct stars (see, e.g., Antoci et al. 2019; Barceló Forteza et al. 2020). Together they present an extensive asteroseismic data set that tests theoretical models of intermediate mass stars and their mode excitation.

These space-based observations help underscore a confounding problem that was already apparent in earlier ground-based observations: δ Sct stars with very similar global parameters often have very different oscillation frequencies and amplitudes (Balona & Dziembowski 2011; Balona 2018, 2021). Most recently, the analysis of the oscillation spectra of 9597 *TESS* δ Sct stars by Balona (2021) finds little, if any, correlation between the frequencies and locations of the stars in the Hertzsprung-Russel diagram. He notes that otherwise similar stars can have frequency rich spectra or be dominated by just one frequency peak. By contrast, non-adiabatic pulsation models predict that stars with similar parameters will exhibit similar oscillation spectra. Balona (2021) concludes that an unknown mode selection process must be active and suggests that the problem may be related to the driving of modes to nonlinear amplitudes.

Another unexplained feature of some δ Sct stars is that their observed mode periods change much faster than evolutionary models predict (Rodríguez et al. 1995; Breger & Pamyatnykh 1998; Rodríguez & Breger 2001; Bowman et al. 2016, 2021). For example, Breger & Pamyatnykh (1998) find linear period changes $\dot{P}/P \simeq 10^{-7} \text{ yr}^{-1}$ in Population I (metal rich) radial pulsators, an order of magnitude faster than expected based on stellar evolution. Moreover, they find an equal distribution of period increases and decreases whereas evolutionary models predict that they should mostly increase. They also find that Population II (metal poor) δ Sct

stars can exhibit very sudden period changes of order $\Delta P/P \simeq 10^{-6}$. Similarly, Bowman et al. (2021) find that the fundamental and first overtone radial modes of the HADS star KIC 5950759 exhibits a linear period change $\dot{P}/P \simeq 10^{-6} \text{ yr}^{-1}$ over a timescale of several years, at least two orders of magnitude larger than predicted by evolutionary models. Both Breger & Pamyatnykh (1998) and Bowman et al. (2021) suggest (see also Blake et al. 2003) that the rapid period changes could be the result of nonlinear mode interactions. Such interactions can enable a fast transfer of energy among the modes and induce rapid, amplitude-dependent variations in their oscillation periods.

Bowman et al. (2016) find further evidence of nonlinear mode interactions in their ensemble study of *Kepler* δ Sct stars. Of the 983 stars they analyze, 603 exhibit at least one pulsation mode that varies significantly in amplitude over four years. While some of these amplitude variations are due to the star being in a binary, they conclude that some must be due to processes intrinsic to the star and that nonlinear mode interactions is a likely culprit. In a detailed analysis of KIC 5892969, Barceló Forteza et al. (2015) likewise report finding amplitude variations that they argue can be attributed to nonlinear mode interactions. Analogous to the Balona (2021) study of *TESS* δ Sct stars cited above, Bowman et al. (2016) find no obvious correlation between the appearance of amplitude variations and stellar parameters such as the surface gravity $\log g$ or T_{eff} .

Somewhat separately, Bowman et al. (2016) note that in many δ Sct stars the visible pulsation mode energy is not conserved over the four year Kepler observations (see also Bowman & Kurtz 2014) and that low-frequency peaks can sometimes be associated with combination frequencies of high-frequency peaks. They propose that this may be due to a transfer of energy via nonlinear mode interactions from visible modes into non-visible modes (angular degree $l \gtrsim 3$) or into the low frequency modes.

Arguably the most definitive observational evidence of nonlinear mode interactions comes from the analysis of the Kepler δ Sct star KIC 8054146 by Breger & Montgomery (2014). From the oscillation spectrum, they identify several mode triplets with properties consistent with the theory of nonlinear three-mode coupling in which two parent modes driven by the κ -mechanism nonlinearly excite a daughter mode. In particular, for each triplet they find that: (i) the frequencies of the modes combine such that the magnitude of their detuning $\Delta_{abc} \equiv \omega_a \pm \omega_b \pm \omega_c$ is very small ($\lesssim 10^{-5}$ times the individual frequencies), (ii) the O – C phase shift of the daughter mode c varies in time as $\phi_c(t) = \phi_a(t) \pm \phi_b(t)$,

and (iii) the daughter’s amplitude varies in proportion to the product of the parents’ amplitudes, i.e., $A_c(t) = \mu A_a(t)A_b(t)$, where the constant μ is a measure of the nonlinear coupling strength.

There are a number of theoretical studies that consider nonlinear mode interactions in pulsating main sequence stars (e.g., Moskalik 1985; Dziembowski & Krolikowska 1985; Dziembowski et al. 1988; Moskalik & Buchler 1990; Buchler et al. 1997; Nowakowski 2005). However, a comprehensive analysis investigating their impact on the oscillation modes in δ Sct stars has not been carried out. In this paper, we take some initial steps towards achieving such a goal. In Section 2, we present the formalism of three-mode coupling and derive the relation between the coupling strength μ and other stellar and mode parameters. In Section 3, we describe our calculational methods including how we search for strongly coupled modes in our δ Sct stellar models. In Section 4, we present the results of our analysis and compare them with the measurements of mode coupling in KIC 8054146. We summarize in Section 5 and discuss how future theoretical work can help further quantify the impact of nonlinear mode coupling in δ Sct stars.

2. Resonant Three-Mode Coupling

The position \mathbf{x} of a fluid element in an unperturbed star is related to its perturbed position \mathbf{x}' at time t via $\mathbf{x}' = \mathbf{x} + \boldsymbol{\xi}(\mathbf{x}, t)$, where $\boldsymbol{\xi}(\mathbf{x}, t)$ is the Lagrangian displacement vector. Since we are interested in computing weakly nonlinear mode interactions, we account for the equation of motion for $\boldsymbol{\xi}(\mathbf{x}, t)$ to second order in perturbation theory

$$\rho \ddot{\boldsymbol{\xi}} = \mathbf{f}_1[\boldsymbol{\xi}] + \mathbf{f}_2[\boldsymbol{\xi}, \boldsymbol{\xi}], \quad (1)$$

where \mathbf{f}_1 and \mathbf{f}_2 are the linear and second order forces, respectively (see Schenk et al. 2001; Weinberg et al. 2012). We solve for $\boldsymbol{\xi}(\mathbf{x}, t)$ by expanding the phase space vector of the displacement in terms of its linear eigenmodes

$$\begin{bmatrix} \boldsymbol{\xi}(\mathbf{x}, t) \\ \dot{\boldsymbol{\xi}}(\mathbf{x}, t) \end{bmatrix} = \sum_a q_a(t) \begin{bmatrix} \boldsymbol{\xi}_a(\mathbf{x}) \\ -i\omega_a \boldsymbol{\xi}_a(\mathbf{x}) \end{bmatrix}, \quad (2)$$

which allows us to recast the equation of motion as a set of nonlinearly coupled equations for the dimensionless amplitudes $q_a(t)$. Here $\boldsymbol{\xi}_a(\mathbf{x})$ and ω_a are the eigenfunctions and eigenfrequencies of a linear eigenmode and the sums are over all quantum numbers a (angular degree l_a , azimuthal number m_a , and radial order n_a) and both frequency signs ($\pm\omega_a$). We neglect stellar rotation

in our analysis¹ and therefore the eigenfunctions are degenerate in m_a . We normalize the eigenfunctions such that

$$2\omega_a^2 \int d^3x \rho |\xi_a|^2 = E_*, \quad (3)$$

where ρ is the density and $E_* = GM^2/R$ is the characteristic energy of a star of mass M and radius R . The energy of a mode is then $E_a = |q_a|^2 E_*$.

Consider a system of three coupled modes, which we label by subscripts a , b , and c . If we plug the expansion given by Equation (2) into Equation (1), use the orthogonality of the eigenfunctions, and add a linear damping term, we obtain an amplitude equation for mode a

$$\dot{q}_a + (i\omega_a + \gamma_a) q_a = i\omega_a \kappa_{abc} q_b^* q_c^*, \quad (4)$$

and similarly for modes b and c . Here asterisks denote complex conjugation, γ_a is the mode's linear damping rate (if $\gamma_a > 0$) or growth rate ($\gamma_a < 0$; in general $\gamma_a > 0$ unless otherwise specified), and κ_{abc} is the three-mode coupling coefficient. The latter is dimensionless and symmetric in the three indices and is found by computing

$$\kappa_{abc} = \frac{1}{E_*} \int d^3x \xi_a \cdot \mathbf{f}_2[\xi_b, \xi_c]. \quad (5)$$

We describe how we calculate γ_a and κ_{abc} in Section 3.

We are interested in a three mode system in which two of the modes are directly excited by the κ -mechanism and the third mode is excited on account of its nonlinear coupling to the other two modes (we assume it is stable to the κ -mechanism). We refer to the former two modes as the parents and label them with subscripts a and b and we refer to the latter mode as the daughter and label it with subscript c . When the magnitude of the triplet's detuning

$$\Delta_{abc} = \omega_a \pm \omega_b \pm \omega_c \quad (6)$$

is small, the parents can potentially drive the daughter to large amplitude. This is a type of nonlinear inhomogeneous driving that [Dziembowski \(1982\)](#) calls direct resonance. Another type of three-mode coupling often

considered in the literature is the parametric instability, which involves one parent resonantly exciting two daughters. Although the parametric instability might also impact the observed power spectra of δ Sct stars, in this paper we will focus on direct resonance. This is because [Breger & Montgomery \(2014\)](#) find strong evidence for direct resonance in their observations of KIC 8054146 and [Bowman et al. \(2016\)](#) argue it can account for the amplitude modulations of many δ Sct stars observed by *Kepler*.

We now calculate the amplitude of a daughter mode $q_c(t)$ excited by direct resonance with two parents. For simplicity, we assume the parent amplitudes are set entirely by the κ -mechanism and we ignore the feedback of the daughter on their amplitudes. This should be a good approximation as long as the parent energies E_a and E_b are larger than the daughter's. Since the parent energies will be nearly constant on the timescale of the oscillations², we can write $q_a(t) = A_a e^{-i(\omega_a t + \delta_a)}$, and similarly for mode b , where the amplitude $A_a = \sqrt{E_a/E_0}$ and the phase lag δ_a are real constants. The daughter's amplitude equation is then just that of a driven harmonic oscillator with forcing frequency $\omega_a + \omega_b$ and driving force $i\omega_c \kappa_{abc} A_a A_b e^{i(\delta_a + \delta_b)}$. Writing $q_c = A_c e^{i[(\omega_a + \omega_b)t + \delta_c]}$, the daughter's amplitude equation then gives

$$(i\Delta_{abc} + \gamma_c) A_c e^{i\delta_c} = i\omega_c \kappa_{abc} A_a A_b e^{i(\delta_a + \delta_b)}. \quad (7)$$

If we multiply each side of this equation by its complex conjugate, we get

$$A_c = \mu A_a A_b, \quad (8)$$

where the nonlinear coupling strength

$$\mu = \frac{|\omega_c \kappa_{abc}|}{\sqrt{\Delta_{abc}^2 + \gamma_c^2}}. \quad (9)$$

If instead we separate Equation (7) into its real and imaginary parts and take their ratio, we get

$$\tan(\delta_a + \delta_b) = \frac{\Delta_{abc} \sin \delta_c - \gamma_c \cos \delta_c}{\Delta_{abc} \cos \delta_c + \gamma_c \sin \delta_c}. \quad (10)$$

We thus see that if $|\Delta_{abc}| \gg \gamma_c$ then $\delta_c \simeq \delta_a + \delta_b$, whereas if $\gamma_c \gg |\Delta_{abc}|$ then $\delta_c \simeq \delta_a + \delta_b - \pi/2$. This is the standard result that for a driven damped harmonic oscillator, the driving and response are in phase if the detuning is large (compared to the damping) and $\pi/2$ out of phase if the detuning is small.

¹ Although some δ Sct stars rotate rapidly (including KIC 8054146), their spin frequencies are typically much less than the frequency of the modes, with the exception, perhaps, of the low frequency g -modes. For example, KIC 8054146 has a measured rotational velocity $v \sin i = 300 \pm 20$ km s⁻¹ and [Breger et al. \(2012\)](#) estimate that its spin frequency is $\simeq 3$ cycles day⁻¹ (corresponding to 70% of its Keplerian breakup frequency). Since this is at least ten times smaller than its p -mode frequencies, we do not expect rotation to drastically modify the eigenfunctions.

² The observed amplitude modulations are on timescales of $\gtrsim 100$ days ([Breger & Montgomery 2014](#); [Bowman et al. 2016](#)) and thus we can treat the parent amplitudes as nearly constant on the timescale of the oscillation periods (\lesssim hours).

Breger & Montgomery (2014) present a similar relation for μ (their equation 5), although it looks slightly different. This is partly because they adopt a different eigenfunction normalization. More importantly, their expression neglects detuning and effectively assumes $|\Delta_{abc}| \ll \gamma_c$. However, we will see that this is not generally true: for the triplets with the largest μ , it is often Δ_{abc} rather than γ_c that limits the magnitude of μ .

3. Computational Methods

In Section 3.1 we describe our δ Sct models and how we solve for their linear eigenmodes and in Section 3.2 we describe how we calculate their linear damping rates. In Section 3.3, we explain our method for calculating the coupling coefficient κ_{abc} . In Section 3.4, we describe our procedure for finding the triplets with the largest coupling strength μ and present a combinatorics argument to understand what sets the minimum detuning.

3.1. Stellar Models and Linear Eigenmodes

We use the MESA stellar evolution code (Paxton et al. 2019) to construct fourteen δ Sct models with masses $M = 1.7, 1.85, 2.0,$ and $2.2M_\odot$ and effective temperatures in the range $7200 \lesssim T_{\text{eff}} \lesssim 8300$ K. In Figure 1, we show the location of our models in the $\log g$ - T_{eff} plane. The diagonal lines show the locations of the observational blue and red edges of the instability strip from Rodríguez & Breger (2001). We constructed our δ Sct models so that they roughly span its range. Figure 1 also shows the location of the δ Sct stars observed by *Kepler* (Bowman et al. 2016).

The observed power spectra of δ Sct stars contain g - and p -modes with frequencies that range from a few cycles day^{-1} (g -modes) to ≈ 100 cycles day^{-1} (p -modes) and angular degree $0 \leq l \lesssim 3$ (modes with $l \gtrsim 3$ cannot typically be resolved by *Kepler*). We use the stellar oscillation code GYRE (Townsend & Teitler 2013; Townsend et al. 2018) to find modes in this range for each of our δ Sct models. Specifically, for each model we find the 160 modes with radial order $-20 \leq n \leq 20$ and angular degree $0 \leq l \leq 3$. For our representative model, the results of which we discuss in Section 4.1, our mode frequencies range from about one to 85 cycles day^{-1} .

In the top panels of Figures 2 and 3 we show the radial displacement profiles $\xi_r(r)$ for a representative p -mode and g -mode, respectively. As expected, the p -mode amplitude peaks near the surface of the star and is orders of magnitude smaller in the deep stellar interior (note that the abscissa in Figure 2 is $R - r$). The g -mode amplitude, by contrast, is nearly uniform throughout the interior. Note too that the g -mode’s wavelength is

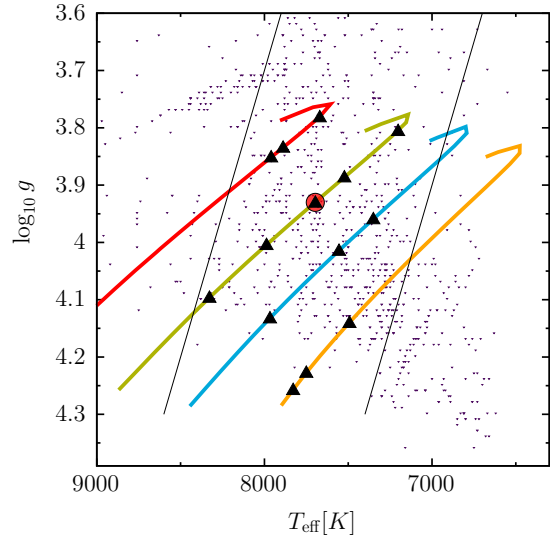


Figure 1. Location of the fourteen δ Sct stellar models (black triangles) on the $\log g$ - T_{eff} plane, with the representative model (Section 4.1) circled in red. The models have mass $M = 1.7, 1.85, 2.0,$ and $2.2M_\odot$ and their evolution are shown by the orange, blue, green, and red curves, respectively. The purple triangles in the background are the *Kepler* δ Sct stars from Bowman et al. (2016) and the diagonal lines are the observational blue and red edges of the classical instability strip.

shortest where the Brunt–Väisälä frequency peaks just outside the convective core at $r \simeq 1.0 \times 10^{10}$ cm and it is evanescent within it. These differences affect the spatial location of the nonlinear mode coupling within the star, as we discuss in Section 3.3.

3.2. Linear Mode Damping

The two principle sources of linear dissipation acting on the oscillation modes are radiative and turbulent damping. The former is due to dissipation of the mode-induced temperature fluctuations by radiative diffusion. The latter is due to dissipation of the mode-induced fluid displacements by turbulent eddies within the convective core.

We calculate the radiative damping rate of a mode $\gamma_a^{(\text{rad})}$ from GYRE’s solution of the nonadiabatic oscillation equations. For all other parts of our calculations (eigenfrequencies, displacements, etc.) we use the solution of the adiabatic oscillation equations.³ In order to assign $\gamma_a^{(\text{rad})}$ to an adiabatic eigenmode, we take its values as a function of the nonadiabatic eigenfrequencies

³ This is primarily because the expressions we use to compute κ_{abc} assume adiabatic eigenmodes. Since the damping rates are all much smaller than the mode frequencies we consider, the modes are adiabatic to a good approximation.

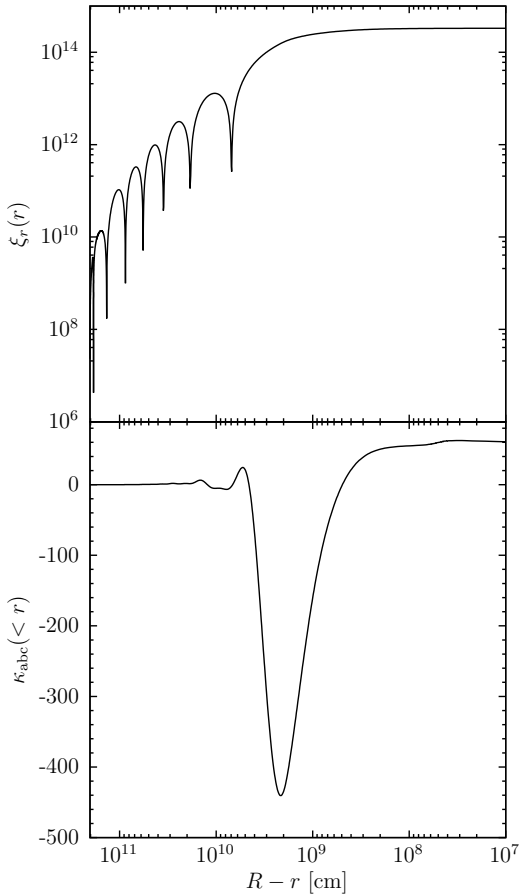


Figure 2. Top panel: Radial displacement ξ_r as a function of depth $R - r$ for an $l_a = 2$, $n_a = 5$ p -mode. Bottom panel: Cumulative integral of the coupling coefficient $\kappa_{abc}(< r)$ for a large μ triplet (see Table 1 in the appendix) that includes the p -mode shown in the top panel. The modes of the triplet have $(l_a, l_b, l_c) = (2, 2, 2)$ and $(n_a, n_b, n_c) = (5, 15, 6)$ and are from the $M = 2.2M_\odot$, $T_{\text{eff}} = 7960$ K model.

and use interpolation to assign it to the adiabatic eigenfrequencies (the two frequencies differ only slightly).

We find the turbulent damping rate by computing

$$\gamma_a^{(\text{turb})} = \frac{\omega_a^2}{E_\star} \int dr \rho r^2 \nu_{\text{turb}} F(r), \quad (11)$$

where $F(r)$ depends on the eigenfunction displacement and is given by the expression found in Higgins & Kopal (1968; see also Lai 1994). The turbulent effective viscosity ν_{turb} depends on the ratio of the convective turnover frequency (provided by MESA) to the mode frequency and is reduced when this ratio is small. To calculate ν_{turb} , we use the power-law expression given in Duguid et al. (2020) from a fit to their numerical simulations.

In Figure 4 we show $\gamma_a^{(\text{rad})}$ and $\gamma_a^{(\text{turb})}$ as a function of mode frequency for all the $l = 2$ modes of the $2.0M_\odot$, 7696 K model (the other models yield similar re-

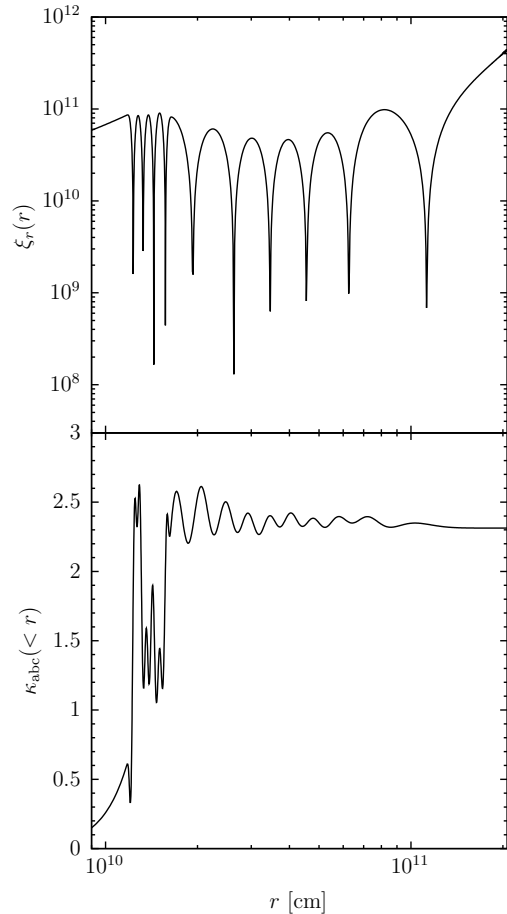


Figure 3. Top panel: Radial displacement ξ_r as a function of radius for an $l_c = 2$, $n_c = -10$ g -mode. Bottom panel: Cumulative integral of the coupling coefficient $\kappa_{abc}(< r)$ for a large μ triplet (see Table 1 in the appendix) that includes the g -mode shown in the top panel. The modes of the triplet have $(l_a, l_b, l_c) = (1, 1, 2)$ and $(n_a, n_b, n_c) = (-13, -11, -10)$ and are from the $M = 2.2M_\odot$, $T_{\text{eff}} = 7888$ K model.

sults). We see that the radiative damping dominates at essentially all frequencies, often by a factor of ~ 100 , and therefore the total damping rate

$$\gamma_a^{(\text{tot})} = \gamma_a^{(\text{rad})} + \gamma_a^{(\text{turb})} \simeq \gamma_a^{(\text{rad})}. \quad (12)$$

The p -mode damping rates are several orders of magnitude larger than the g -mode damping rates because the p -modes have much smaller mode inertias (see Aerts et al. 2010). Moreover, since the efficiency of radiative dissipation increases with decreasing wavelength, we see that $\gamma_a^{(\text{rad})}$ increases with increasing p -mode frequency and decreasing g -mode frequency.

3.3. Nonlinear coupling coefficient κ_{abc}

We calculate κ_{abc} using Equations A55 through A62 in Weinberg et al. (2012). The modes couple only if

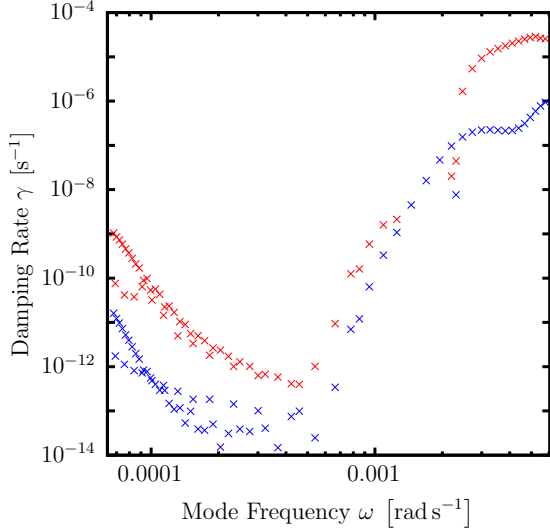


Figure 4. Linear mode damping rate due to radiative (red points) and turbulent (blue points) dissipation as a function of mode frequency for the $l = 2$ modes of our representative δ Sct model ($M = 2.0M_{\odot}$, $T_{\text{eff}} = 7696$ K, $\log g = 3.9$).

they satisfy the angular selection rules $|\ell_b - \ell_c| \leq \ell_a \leq \ell_b + \ell_c$ with $\ell_a + \ell_b + \ell_c$ even and $m_a + m_b + m_c = 0$. The angular selection rules help restrict the number of triplets to consider in our search for large μ values. In Section 4 we show that the triplets with the largest μ have $\kappa_{abc} \sim 1 - 100$.

As representative examples of the κ_{abc} calculation, in Figure 2 we show the cumulative integral $\kappa_{abc}(< r) = \int_0^r (d\kappa_{abc}/dr) dr$ for a triplet of three p -modes and in Figure 3 for a triplet of three g -modes. For the triplet shown in Figure 2, $\kappa_{abc} \simeq 60$ and most of the contribution to κ_{abc} (i.e., most of the nonlinear coupling) occurs in the outer layers of the star. This triplet has fractional detuning $\Delta_{abc}/\omega_c \simeq 1.3 \times 10^{-4}$, $\gamma_c = 9.9 \times 10^{-8} \text{ s}^{-1}$, and $\mu = 3.7 \times 10^5$. For the triplet shown in Figure 3, $\kappa_{abc} \simeq 2.3$ and most of the contribution occurs in the deep interior just outside the convective-radiative interface. This is because that is where the mode amplitudes of the respective triplets peak. This triplet has $\Delta_{abc}/\omega_c \simeq 3.0 \times 10^{-7}$, $\gamma_c = 1.0 \times 10^{-12} \text{ s}^{-1}$, and $\mu = 7.6 \times 10^6$.

3.4. Search for triplets with large coupling strength μ

We are interested in finding the triplets with the largest values of the nonlinear coupling strength μ . From Equation (9), we see this requires finding triplets with large κ_{abc} and small Δ_{abc}/ω_c and γ_c/ω_c . For each of our δ Sct models, we search for the triplets with the largest μ by scanning over all combinations of mode triplets among our sample of 160 modes. Since com-

puting κ_{abc} is the most expensive part of the μ calculation, we restrict our search to triplets with detuning $|\Delta_{abc}| < 0.15\sqrt{GM/R^3}$. In practice, this does not affect our results since the largest μ all have much smaller detunings than this. As we show in Section 3.4.1, the magnitude of the smallest detunings can be understood as resulting from the repeated drawing of three random numbers from a uniform distribution. Note that when calculating Δ_{abc} , we must account for all combinations of mode frequency signs (see Equation 6) since the phase space mode expansion includes both positive and negative frequencies for each ω_a . This means that the daughters are not necessarily the highest frequency mode of the triplet; indeed, for many of our largest μ they are the intermediate frequency mode (Breger et al. 2012 find this as well among the triplets they identify in KIC 8054146).

3.4.1. Minimum detuning Δ_{abc}

In Section 4 we show that all of our δ Sct models have minimum fractional detunings $\Delta_{abc}/\omega_c \approx 10^{-5}$. We can roughly understand what sets this minimum as follows. For each model, the mode frequencies lie between some minimum and maximum, $\omega_{\min} \leq \omega_a \leq \omega_{\max}$, corresponding to the highest order g - and p -modes. To a reasonable approximation, we can treat the 160 calculated modes from each model as though their frequencies are uniformly distributed between these two values.⁴ Assume, therefore, that $a \equiv (\omega_a - \omega_{\min}) / (\omega_{\max} - \omega_{\min})$ is uniformly distributed between 0 and 1, and write $\Delta_{abc} = \omega_a + \omega_b - \omega_c$ as $\epsilon = a + b - c$, where $\epsilon \equiv (\Delta_{abc} - \omega_{\min}) / (\omega_{\max} - \omega_{\min})$ is similar to the fractional detuning Δ_{abc}/ω_c . For a random draw of $\{a, b, c\}$, the probability $P(|\epsilon| < \epsilon_0) = \epsilon_0 - \epsilon_0^2/4 \simeq \epsilon_0$ for $0 < \epsilon_0 \ll 1$.⁵ On average, we therefore need $\simeq 1/\epsilon_0$ draws of $\{a, b, c\}$ before we get an $|\epsilon| < \epsilon_0$. For $0 \leq l \leq 3$, there are eight combinations of $\{l_a, l_b, l_c\}$ that satisfy the selection rules (see Section 3.3) and since $-20 \leq n \leq 20$, there are about $\binom{40}{3} \simeq 10^4$ combinations of $\{n_a, n_b, n_c\}$. Our search therefore has $\approx 10^5$ unique combinations of $\{a, b, c\}$ and we can expect a minimum $|\epsilon| \approx 10^{-5}$, consistent with our calculated minimum Δ_{abc}/ω_c .

Breger & Montgomery (2014) find that the triplets in KIC 8054146 have fractional detunings $\lesssim 10^{-6}$, somewhat smaller than our calculated minimum. This could

⁴ Since the modes are relatively low-order, they do not satisfy the asymptotic relations appropriate for high-order modes, in which the period (g -modes) or frequency (p -modes) spacings are nearly constant for fixed l .

⁵ An approximate way to understand this is that there is a 50% chance $a + b < 1$. If it is, there is a $2\epsilon_0$ chance that c will be within ϵ_0 of $a + b$ and therefore $P(|\epsilon| < \epsilon_0) \simeq \epsilon_0$.

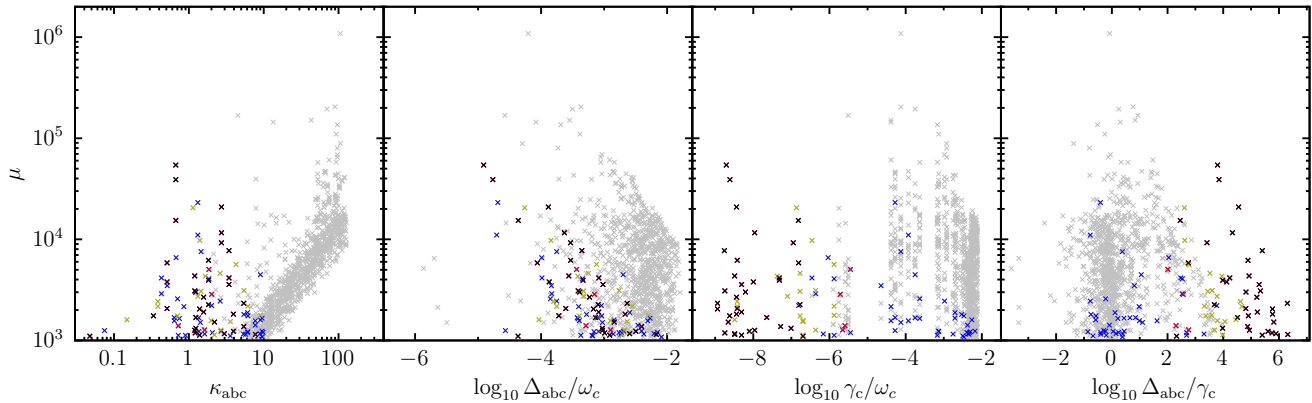


Figure 5. Triplets with nonlinear coupling strength $\mu > 10^3$ from the $M = 2.0M_{\odot}$, $T_{\text{eff}} = 7696$ K, model. The panels show μ as a function of the coupling coefficient κ_{abc} , the fractional detuning Δ_{abc}/ω_c , the daughter damping rate γ_c (in units of ω_c), and the ratio Δ_{abc}/γ_c . The different colors correspond to different triplet types: three p -modes (grey points), three g -modes (black points), two p -mode parents and a g -mode daughter (green points), two g -mode parents and a p -mode daughter (red points), one parent a p -mode and the other a g -mode (blue points; the daughter can be either a p - or g -mode).

be because we do not account for rotation, which lifts the degeneracy in m_a . It therefore increases the total number of unique triplet combinations and further reduces the minimum Δ_{abc}/ω_c .

4. Results

In Section 4.1, we show results for a representative δ Sct model with $M = 2.0M_{\odot}$, $T_{\text{eff}} = 7696$ K, and $\log g = 3.9$. We choose this model because it lies near the middle of the instability strip (see Figure 1) and because KIC 8054146 has similar T_{eff} and $\log g$ (Breger et al. 2012; Breger & Montgomery 2014). In Section 4.2, we show results for our other δ Sct models, which we find are generally similar to those of our representative model. In Section 4.3 we compare our results to the triplets identified in KIC 8054146.

4.1. Representative δ Sct model

In Figure 5, we show the triplets with the largest coupling strengths μ from our representative model ($M = 2.0M_{\odot}$, $T_{\text{eff}} = 7696$ K, $\log g = 3.9$). We see that there are many triplets with $\mu > 10^4$ and even a few with $\mu > 10^5$. The four panels, from left to right, show how μ depends on the coupling coefficient κ_{abc} , the fractional detuning Δ_{abc}/ω_c , the daughter damping rate γ_c/ω_c , and Δ_{abc}/γ_c . Although the coupling strength can be as large as $\mu \sim 10^4$ even for coupling coefficients as small as $\kappa_{abc} \approx 1$, the largest μ tend to have $\kappa_{abc} \gtrsim 10$. These are generally the triplets containing three p -modes (grey points). Nonetheless, other types of triplets involving different combinations of p - and g -modes (colored points) can still have $\mu \gtrsim 10^3$. The second panel shows that the largest μ are more likely to have small detunings, with $\Delta_{abc}/\omega_c \lesssim 10^{-3}$ (in Section 3.4.1 we explain why the minimum $\Delta_{abc}/\omega_c \approx 10^{-5}$). By contrast,

the third panel shows that the largest μ are not especially sensitive to γ_c ; if anything they are more likely to have larger γ_c (those are the ones in which the daughter is a p -mode; see Figure 4). This is because for the majority of strongly coupled triplets $\Delta_{abc} \gtrsim \gamma_c$, as can be seen in the fourth panel. Thus, by Equation (9), μ tends to be limited by the magnitude of Δ_{abc} rather than γ_c .

In Figure 6 we show (in red) the amplitude of the daughter modes $A_c = |q_c|$ as a function of their frequency for the representative δ Sct model. This figure is like a power-spectrum, albeit a fairly artificial one. Specifically, to calculate A_c we use Equation (8) assuming the parents (in blue) are all at amplitude $A_a = A_b = 10^{-6}$. While this choice of parent amplitude is essentially arbitrary (the actual amplitudes are set by the κ -mechanism driving of the parents, which we do not attempt to model), the reason we choose $A_a = A_b = 10^{-6}$ is because then the best coupled triplets ($\mu \sim 10^5$) have $A_c \sim 10^{-7}$ to 10^{-6} . Thus, our choice ensures the daughter amplitudes are comparable to their parents' amplitudes, which is similar to the daughter modes observed in KIC 8054146 (Breger & Montgomery 2014). Interestingly, we see in Figure 6 that while most of the high amplitude daughters are p -modes (frequencies greater than about 15 cycles day $^{-1}$; see black vertical line), the g -mode daughters can also have significant amplitudes. This too is a feature observed in KIC 8054146.

A notable difference between our artificial power spectrum (Fig. 6) and the observed power spectrum of KIC 8054146 (see Fig. 1 in Breger & Montgomery 2014) is that ours has a much higher density (per unit frequency) of parent and daughter modes with large amplitudes. Although we do not know for certain, we suspect that this is because in our treatment we assume every p - and

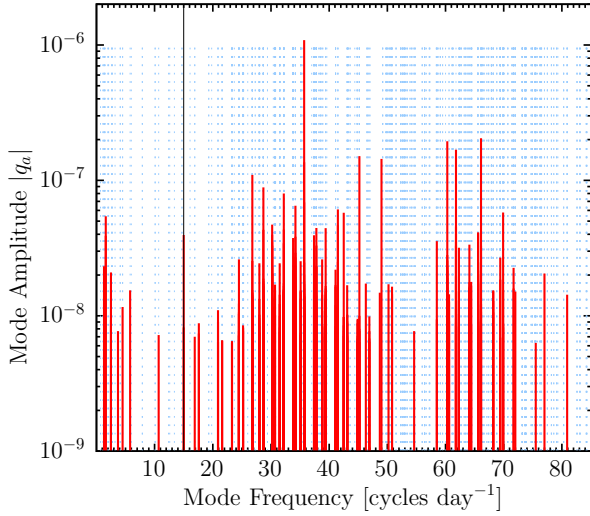


Figure 6. Mode amplitude as a function of frequency for triplets of the $M = 2.0M_{\odot}$, $T_{\text{eff}} = 7696$ K model. The parents (blue lines) are assumed to be at a fixed amplitude $A_a = A_b = 10^{-6}$. The daughters (red lines) are at amplitude $A_c = \mu A_a A_b$. Only triplets with $\mu > 10^3$ are shown. The black line indicates the dynamical frequency $\sqrt{GM/R^3}$ which approximately separates the p - and g -modes.

g -mode parent is unstable to the κ -mechanism and linearly driven to $A_a = A_b = 10^{-6}$. In reality, as the power spectrum of KIC 8054146 indicates, only a subset of these modes will be linearly unstable and driven to sufficiently large amplitudes to be detectable⁶ (and to likewise drive daughters to detectable amplitudes).

In order to determine which modes are unstable to the κ -mechanism, we could turn to GYRE’s solution of the nonadiabatic oscillation equations and find which modes have $\gamma_a^{(\text{rad})} < 0$. Goldstein & Townsend (2020) use this approach to find the unstable modes in models of β Cephei stars whose oscillations are driven by the iron-bump κ -mechanism. However, in practice we find that only low-order modes with $n \approx \text{few}$ have $\gamma_a^{(\text{rad})} < 0$. Moreover, when we include turbulent dissipation $\gamma_a^{(\text{turb})}$, which GYRE does not account for, many of these modes have total damping $\gamma_a^{(\text{tot})} > 0$. Compared to the observed spectra of δ Sct stars, GYRE seems to find too few unstable modes and the range of frequencies is too low ($f \lesssim 40$ cycles day⁻¹). The origin of this discrepancy is unclear, though it could be related to the larger problem of the unknown mode selection process noted in the introduction.

⁶ Note, however, that Breger & Montgomery (2014) only analyze the twenty dominant modes and their harmonics. The full spectrum presented in Breger et al. (2012) contains many more modes.

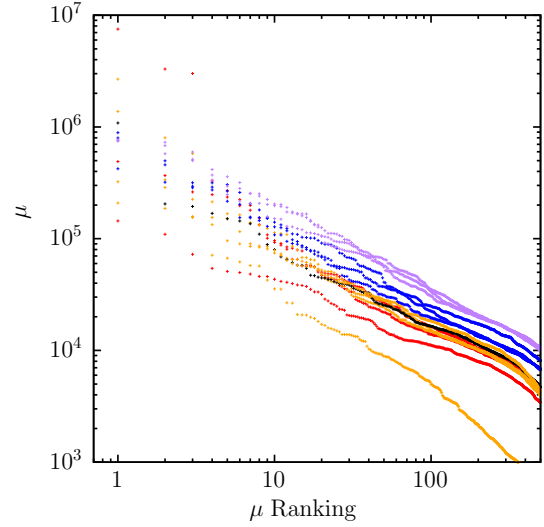


Figure 7. Rank ordering of triplets according to their non-linear coupling strength μ for the fourteen δ Sct models. The points are colored according to the stellar mass: $M = 2.2M_{\odot}$ (red), $M = 2.0M_{\odot}$ (orange with the representative model in black), $M = 1.85M_{\odot}$ (blue), and $M = 1.7M_{\odot}$ (purple).

This important caveat aside, we find two triplets whose parents are both unstable according to GYRE ($\gamma_a^{(\text{tot})} < 0$) and whose μ is large enough ($\mu \simeq 10^4$) to drive a daughter to significant amplitude (again assuming $A_a = A_b = 10^{-6}$). These two triplets are listed in Table 1 in the appendix (see the lines starting with asterisks among the triplets of the representative model).

4.2. Our other δ Sct models

In Figure 7 we show the largest μ triplets in rank order for each of our fourteen δ Sct models. We find that all the models, save one, have more than one hundred triplets with $\mu > 10^4$ and a few triplets with $\mu > 10^5$. Triplets with strong nonlinear coupling are thus a common feature of our δ Sct models.

In Table 1 in the appendix we provide more detailed information about the triplets with the three largest μ for each model. Most of these triplets consist of three p -modes, although some consist of three g -modes or a mix of p - and g -modes. With only a few exceptions, the daughter is either the lowest frequency or intermediate frequency mode of the triplet. While high-frequency daughters tend not to be among the highest- μ triplets (those with $\mu \sim 10^4 - 10^5$), Figure 8 shows that the triplets with $\mu \sim 10^3$ often do contain high-frequency, high-order, p -mode daughters ($f \gtrsim 60$ cycles day⁻¹, $n \gtrsim 10$). It also shows that they sometimes contain low-frequency g -mode daughters ($f \lesssim 15$ cycles day⁻¹, $n < 0$) despite their somewhat smaller κ_{abc} (see Fig. 5).

As with the representative model, we also list in Table 1 the two largest μ triplets whose parents are both unstable, i.e., $\gamma_a^{(\text{tot})} < 0$ according to GYRE (not all models have such triplets). In general, they consist of low-order modes and have $\mu \gtrsim 10^3$.

4.3. Comparison to the δ Sct star KIC 8054146

The stellar parameters of our representative δ Sct model ($M = 2.0M_\odot$, $T_{\text{eff}} = 7696$ K, and $\log g = 3.9$) are similar to those of the Kepler δ Sct star KIC 8054146 studied by Breger & Montgomery (2014). They found several resonant triplets in their analysis of the star’s power spectrum, and focus on three of them in particular. Their frequencies (f_a, f_b, f_c) in units of cycles day^{-1} are (25.9509, 60.4346, 34.4836), (25.9509, 63.3680, 37.4170), and (25.9509, 66.2988, 40.3479). All three share a common mode ($f_a = 25.9509 \text{ cycles day}^{-1}$) and to the precision provided in the paper they have detunings $|f_a - f_b + f_c| < 10^{-4} \text{ cycles day}^{-1}$ corresponding to fractional detunings $|\Delta_{abc}|/f_c < 3 \times 10^{-6}$ (given the four year data set, the frequencies cannot be measured to better than $\sim 10^{-4} \text{ cycles day}^{-1}$ and only an upper-bound can be placed on the detunings). They find that the amplitudes vary over the four-year Kepler observations according to Equation (8). This allows them to identify the parent and daughter modes in each triplet since they are observed to vary in concert as $A_c(t) = \mu A_a(t)A_b(t)$. Consistent with the mode coupling interpretation, they also find that their phase shifts vary as $\phi_c(t) = \phi_a(t) \pm \phi_b(t)$. The daughter is the intermediate frequency mode in all three triplets (mode f_c in the list above) and from its amplitude variation they measure a coupling strength in the range $7000 \lesssim \mu \lesssim 60,000$.

This range of measured μ is consistent with the values we find in our calculations (not counting the few triplets we find with $\mu \gtrsim 10^5$). Moreover, as can be seen from Table 1 in the the appendix, our representative δ Sct model contains triplets whose other properties are similar to those found in KIC 8054146, especially the triplet with the third largest μ in the list. Specifically, their frequencies and detunings are similar and since $|\Delta_{abc}| > \gamma_c$, we expect their phase shift, like the phase lag, to satisfy $\phi_c \simeq \phi_a \pm \phi_b$ (see Section 2). Some of the triplets in KIC 8054146 also contain and a mix of p - and g -modes, like ours. However, given that we find hundreds of triplets with $\mu \gtrsim 10^4$, this similarity between the largest μ triplets listed in Table 1 and those observed in KIC 8054146 could just be a coincidence. As we discuss below, a more definitive comparison requires a time-dependent mode network calculation that also models the parent driving.

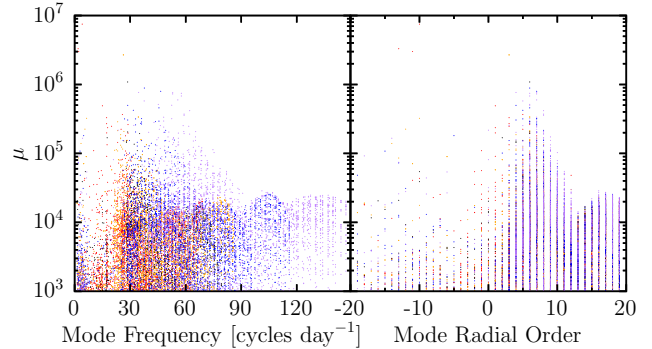


Figure 8. Nonlinear coupling strength μ as a function of daughter mode frequency (left panel) and radial order (right panel) for the fourteen δ Sct models. The points are colored according to the stellar mass (as in Fig. 7): $M = 2.2M_\odot$ (red), $M = 2.0M_\odot$ (orange with the representative model in black), $M = 1.85M_\odot$ (blue), and $M = 1.7M_\odot$ (purple).

5. Summary and Conclusions

Motivated by the observational evidence of nonlinear mode interactions in δ Sct stars, especially in KIC 8054146, we carried out a theoretical investigation of the prevalence and strength of resonant three-mode coupling in fourteen models of δ Sct stars that span the instability strip. For each model, we found all the eigenmodes with angular degree $0 \leq l \leq 3$ and radial order $-20 \leq n \leq 20$, corresponding to g - and p -modes with frequencies in the range $1 \lesssim f \lesssim 100 \text{ cycles day}^{-1}$. We computed the linear damping rate γ of each mode due to radiative and turbulent dissipation and found that the former typically dominates. We then searched for all mode triplets (a, b, c) that satisfy the three-mode angular selection rules and computed their detuning $\Delta_{abc} = \omega_a \pm \omega_b \pm \omega_c$ and coupling coefficient κ_{abc} . Lastly, we rank-ordered the triplets according to their nonlinear coupling strength $\mu = |\omega_c \kappa_{abc}| / \sqrt{\Delta_{abc}^2 + \gamma_c^2}$.

According to the theory of nonlinear three-mode coupling, two parent modes a and b driven by the κ -mechanism to amplitudes A_a and A_b will excite a daughter mode c to an amplitude $A_c = \mu A_a A_b$. In all of our models, we found at least ten triplets with $\mu \gtrsim 10^4$, and in many models there were > 100 such triplets. These μ values are broadly consistent with those directly measured by Breger & Montgomery (2014) in their analysis of KIC 8054146. We found that the triplets with large μ consist of various combinations of p - and g -modes (e.g., three p -modes, three g -modes, two p -mode parents and a g -mode daughter), which is also true of the triplets found in KIC 8054146.

Our results suggest that resonant three-mode interactions can be significant in δ Sct stars, and the ubiquity

of large μ across all of our models may explain why amplitude variations (Bowman et al. 2016) and large \dot{P}/P (Breger & Pamyatnykh 1998; Blake et al. 2003; Bowman et al. 2021) are commonly observed. However, our analysis did not model the parent driving and therefore did not solve for the overall mode amplitudes. Thus, we cannot yet say the extent to which mode coupling impacts the observed oscillation spectra. Moreover, we only focused on direct nonlinear forcing, in which two parent modes excite a daughter mode. Another form of three-mode coupling that might impact the oscillation spectra is the parametric instability, in which a parent mode excites two daughter modes (see, e.g., Dziembowski 1982). Unlike direct forcing, the parametric instability is only triggered if a parent is above a threshold amplitude. Dziembowski & Krolikowska (1985) showed that it is a potentially important mechanism for limiting oscillation amplitudes and transferring energy across the modes (see also Dziembowski et al. 1988). A further complication is that the daughters can themselves excite granddaughters and the granddaughters can excite great-granddaughters etc., either through direct forcing, the parametric instability, or both.

In order to make further progress on this problem, a time-dependent mode network calculation is needed. This would entail solving a large set of nonlinearly coupled amplitude equations that account for the parent driving, multiple generations of p - and g -modes, and both forms of three-mode coupling. Weinberg et al.

(2021; see also Weinberg & Arras 2019) carried out a similar calculation in their study of solar-like oscillations in red giants, although there the parents were driven by stochastic turbulent motions not the κ -mechanism. They found that depending on the evolutionary state of the red giant, the secondary modes (daughters, granddaughters, etc.) could significantly suppress the parent amplitudes and efficiently transfer the parents' energy among thousands of higher-order, higher-degree modes. The structure of a red giant, and therefore the mode coupling, is of course very different from that of a δ Sct star. Most notably, the nonlinear mode interactions in a red giant are concentrated in the stellar core and involve mixed modes. In a δ Sct star, by contrast, we found that many of the triplets consist of three p -modes whose nonlinear couplings peak near the stellar surface. Such surface interactions might impact the oscillation spectra more directly and leave a detectable, time-dependent imprint on not just the mode amplitudes, but also on their frequencies and line widths.

This work was supported by NASA ATP grant 80NSSC21K0493. We thank Phil Arras and Hang Yu for valuable discussions.

Software: MESA (Paxton et al. 2019, <http://mesa.sourceforge.net>), GYRE (Townsend & Teitler 2013; Townsend et al. 2018, <https://gyre.readthedocs.io/en/stable/>)

APPENDIX

A. TABLE OF TRIPLETS WITH LARGE NONLINEAR COUPLING STRENGTH

Table 1. Triplets with the largest values of the nonlinear coupling strength μ from each δ Sct model. The subscripts a and b label the parents and subscript c labels the daughter. The columns are: angular degree l , radial order n , mode frequency f (in cycles day⁻¹), total damping rate (in units of $\log_{10} \gamma^{(\text{tot})}/\omega_c$), frequency detuning (in units of $\log_{10} \Delta_{abc}/\omega_c$), coupling coefficient κ_{abc} , and $\log_{10} \mu$. For each model, the first three rows show the largest μ triplets. The following two rows (indicated by asterisks) show the largest μ triplets whose parents both have negative damping rates (we then give $\log_{10}[-\gamma_a^{(\text{tot})}/\omega_c]$; note that not all models have such triplets). Two of the triplets containing three g -modes repeat with different parent-daughter combinations, and we only list the one with the largest μ .

l_a	l_b	l_c	n_a	n_b	n_c	f_a	f_b	f_c	$\log \gamma_a$	$\log \gamma_b$	$\log \gamma_c$	$\log \Delta_{abc}$	κ_{abc}	$\log \mu$
$M = 2.2M_{\odot}, T_{\text{eff}} = 7670 \text{ K}, \log g = 3.78$														
3	3	0	19	10	7	61	38	23	-1.9	-2.0	-3.5	-4.6	-46.3	5.2
0	1	1	17	13	-1	52	41	10	-1.6	-1.5	-6.1	-4.7	2.1	5.0
0	3	3	8	15	5	26	50	24	-2.7	-1.9	-3.0	-4.5	77.8	4.9
* 3	2	1	2	4	12	19	20	39	-5.0	-5.3	-2.2	-2.2	49.7	3.7
* 1	2	1	4	4	12	18	20	39	-5.2	-5.3	-2.2	-3.1	34.5	3.7
$M = 2.2M_{\odot}, T_{\text{eff}} = 7888 \text{ K}, \log g = 3.83$														
1	1	2	-13	-11	-10	2	2	4	-7.1	-6.6	-8.5	-6.5	2.3	6.9
3	2	1	4	11	3	23	40	17	-5.0	-1.9	-4.8	-4.2	21.5	5.5

2	1	1	6	13	3	28	45	17	-3.1	-1.8	-4.8	-3.9	30.7	5.4
* 3	2	1	4	4	13	23	22	45	-5.4	-5.1	-2.2	-2.7	64.5	4.0
* 0	1	1	6	5	-14	23	21	2	-3.7	-4.3	-6.0	-2.1	0.8	2.0
$M = 2.2M_{\odot}, T_{\text{eff}} = 7960 \text{ K}, \log g = 3.85$														
0	2	2	6	10	1	23	38	15	-4.9	-2.0	-4.9	-4.8	9.3	5.7
2	2	2	6	15	5	29	55	26	-3.7	-2.0	-4.3	-3.8	59.8	5.6
2	2	2	15	5	6	55	26	29	-2.0	-4.3	-3.7	-3.9	59.8	5.4
* 3	1	2	4	6	13	24	25	48	-5.5	-6.9	-2.2	-2.4	75.2	4.0
* 3	2	1	4	4	13	24	23	47	-5.5	-5.6	-2.2	-2.5	63.0	3.9
$M = 2.0M_{\odot}, T_{\text{eff}} = 7202 \text{ K}, \log g = 3.80$														
3	0	3	4	4	-10	23	17	6.5	-4.7	-4.6	-8.8	-6.5	-0.1	5.5
1	0	1	7	15	6	26	49	23	-2.7	-1.8	-3.5	-3.7	109.0	5.5
1	2	3	-13	-14	-12	2	3	6	-6.4	-8.4	-8.6	-5.3	-1.1	5.4
* 0	2	2	3	-2	-17	14	11	3	-4.6	-5.7	-8.0	-4.5	0.4	4.1
* 3	1	2	0	3	8	16	17	33	-5.7	-5.3	-2.5	-2.7	6.5	3.3
$M = 2.0M_{\odot}, T_{\text{eff}} = 7523 \text{ K}, \log g = 3.89$														
2	1	1	16	9	6	63	37	27	-1.8	-2.4	-3.8	-3.5	77.7	5.3
2	2	2	8	15	4	35	60	25	-2.8	-1.7	-4.3	-3.5	57.4	5.3
2	2	0	17	9	7	67	38	29	-1.8	-2.4	-3.4	-4.5	64.2	5.2
* 2	1	1	2	4	-15	19	20	2	-4.5	-4.2	-7.5	-3.5	0.5	3.2
* 3	0	3	0	5	8	17	22	40	-7.5	-5.7	-3.7	-2.3	4.6	3.0
$M = 2.0M_{\odot}, T_{\text{eff}} = 7696 \text{ K}, \log g = 3.93$														
0	1	1	16	8	6	64	36	29	-1.8	-2.8	-4.1	-4.2	105.7	6.0
2	1	1	8	16	6	37	66	29	-2.6	-1.8	-4.1	-3.4	89.6	5.3
1	2	3	5	14	6	25	60	35	-5.3	-2.0	-3.8	-3.5	70.0	5.3
* 3	3	0	3	3	12	25	25	49	-5.4	-5.4	-2.3	-2.6	30.4	3.7
* 3	3	2	3	3	11	25	25	49	-5.4	-5.4	-2.4	-2.4	18.7	3.5
$M = 2.0M_{\odot}, T_{\text{eff}} = 7987 \text{ K}, \log g = 4.00$														
0	2	2	17	10	3	77	51	26	-1.8	-2.1	-5.2	-4.8	44.6	6.4
1	1	2	17	9	6	79	45	34	-2.0	-2.7	-4.4	-3.6	84.3	5.5
2	3	3	7	15	6	38	74	36	-2.9	-1.9	-3.6	-3.4	72.3	5.2
* 3	2	1	4	5	13	32	31	62	-5.3	-5.4	-2.2	-2.1	51.9	3.7
* 3	3	2	4	4	13	32	32	64	-5.3	-5.3	-2.2	-2.4	38.9	3.7
$M = 2.0M_{\odot}, T_{\text{eff}} = 8328 \text{ K}, \log g = 4.10$														
1	1	2	-13	-18	-13	2	1	3	-8.0	-7.0	-7.9	-5.8	2.4	6.1
1	2	3	15	5	7	82	36	47	-2.0	-4.8	-3.5	-3.0	70.4	4.9
1	3	2	15	8	4	82	52	31	-1.8	-3.0	-4.6	-3.2	46.7	4.8
$M = 1.85M_{\odot}, T_{\text{eff}} = 7350 \text{ K}, \log g = 3.96$														
0	3	3	7	15	6	33	71	38	-3.4	-1.9	-3.9	-4.3	132.7	5.9
2	0	2	17	11	4	77	49	29	-1.8	-2.2	-4.0	-3.9	73.1	5.7
3	3	0	6	15	7	38	71	33	-3.8	-1.8	-3.4	-4.2	132.7	5.5
* 0	2	2	2	-1	4	15	14	29	-6.6	-7.1	-4.0	-3.4	1.3	3.5
* 1	2	3	1	1	5	15	19	34	-6.5	-6.2	-3.8	-3.5	1.1	3.5
$M = 1.85M_{\odot}, T_{\text{eff}} = 7555 \text{ K}, \log g = 4.01$														
1	1	2	19	12	5	92	60	32	-1.7	-2.0	-4.3	-4.3	31.2	5.6
0	0	0	18	10	7	85	49	36	-1.8	-2.4	-3.5	-4.3	102.7	5.5
3	3	0	16	8	7	82	46	36	-1.8	-2.5	-3.5	-3.6	121.2	5.5
* 3	3	0	2	2	10	25	25	49	-6.7	-6.7	-2.5	-2.1	5.3	2.8
* 0	0	0	3	4	9	20	24	45	-7.1	-6.4	-2.7	-4.0	1.0	2.7

$M = 1.85M_{\odot}, T_{\text{eff}} = 7967 \text{ K}, \log g = 4.13$														
2	1	1	8	17	7	54	100	47	-3.0	-1.9	-3.8	-4.3	123.4	5.9
3	0	3	18	11	6	111	65	46	-2.0	-2.4	-4.0	-3.9	80.6	5.7
3	0	3	19	12	6	116	70	46	-2.0	-2.2	-4.0	-4.3	35.7	5.5
$M = 1.7M_{\odot}, T_{\text{eff}} = 7492 \text{ K}, \log g = 4.14$														
3	3	2	17	11	4	109	75	35	-1.7	-2.1	-5.0	-4.4	30.3	5.9
1	2	1	17	10	5	104	67	38	-1.8	-2.3	-4.5	-3.9	70.0	5.8
1	1	2	16	8	6	99	53	45	-1.9	-3.0	-3.6	-4.1	122.3	5.7
* 2	1	1	2	-1	-2	27	16	11	-7.2	-7.5	-9.0	-4.1	-0.4	3.7
* 2	2	2	-2	1	5	15	25	40	-8.9	-6.8	-4.2	-4.1	0.4	3.6
$M = 1.7M_{\odot}, T_{\text{eff}} = 7750 \text{ K}, \log g = 4.23$														
0	0	0	19	11	7	131	78	53	-1.8	-2.4	-3.8	-4.2	120.1	5.9
3	3	0	18	10	7	133	80	53	-1.8	-2.4	-3.8	-4.3	113.4	5.9
2	0	2	7	16	6	59	111	53	-3.3	-1.9	-3.9	-3.7	111.4	5.7
$M = 1.7M_{\odot}, T_{\text{eff}} = 7829 \text{ K}, \log g = 4.26$														
3	0	3	18	11	6	140	82	58	-1.8	-2.5	-3.8	-4.3	129.5	5.9
2	1	3	16	8	6	123	65	58	-1.9	-3.2	-3.8	-4.3	118.1	5.8
3	3	0	19	11	7	147	91	56	-1.8	-2.3	-3.9	-4.0	87.8	5.8

REFERENCES

- Aerts, C. 2021, *Reviews of Modern Physics*, 93, 015001, doi: [10.1103/RevModPhys.93.015001](https://doi.org/10.1103/RevModPhys.93.015001)
- Aerts, C., Christensen-Dalsgaard, J., & Kurtz, D. W. 2010, *Asteroseismology*
- Antoci, V., Cunha, M. S., Bowman, D. M., et al. 2019, *Monthly Notices of the Royal Astronomical Society*, 490, 4040, doi: [10.1093/mnras/stz2787](https://doi.org/10.1093/mnras/stz2787)
- Balona, L. A. 2018, *Monthly Notices of the Royal Astronomical Society*, 479, 183, doi: [10.1093/mnras/sty1511](https://doi.org/10.1093/mnras/sty1511)
- . 2021, arXiv e-prints, arXiv:2109.12574, <https://arxiv.org/abs/2109.12574>
- Balona, L. A., & Dziembowski, W. A. 2011, *Monthly Notices of the Royal Astronomical Society*, 417, 591, doi: [10.1111/j.1365-2966.2011.19301.x](https://doi.org/10.1111/j.1365-2966.2011.19301.x)
- Barceló Forteza, S., Michel, E., Roca Cortés, T., & García, R. A. 2015, *A&A*, 579, A133, doi: [10.1051/0004-6361/201425507](https://doi.org/10.1051/0004-6361/201425507)
- Barceló Forteza, S., Moya, A., Barrado, D., et al. 2020, *Astronomy and Astrophysics*, 638, A59, doi: [10.1051/0004-6361/201937262](https://doi.org/10.1051/0004-6361/201937262)
- Blake, C., Fox, D. W., Park, H. S., & Williams, G. G. 2003, *Astronomy and Astrophysics*, 399, 365, doi: [10.1051/0004-6361:20021676](https://doi.org/10.1051/0004-6361:20021676)
- Bowman, D. M., Hermans, J., Daszyńska-Daszkiewicz, J., et al. 2021, *MNRAS*, 504, 4039, doi: [10.1093/mnras/stab1124](https://doi.org/10.1093/mnras/stab1124)
- Bowman, D. M., & Kurtz, D. W. 2014, *Monthly Notices of the Royal Astronomical Society*, 444, 1909, doi: [10.1093/mnras/stu1583](https://doi.org/10.1093/mnras/stu1583)
- . 2018, *Monthly Notices of the Royal Astronomical Society*, 476, 3169, doi: [10.1093/mnras/sty449](https://doi.org/10.1093/mnras/sty449)
- Bowman, D. M., Kurtz, D. W., Breger, M., Murphy, S. J., & Holdsworth, D. L. 2016, *MNRAS*, 460, 1970, doi: [10.1093/mnras/stw1153](https://doi.org/10.1093/mnras/stw1153)
- Breger, M. 2000, in *Astronomical Society of the Pacific Conference Series*, Vol. 210, *Delta Scuti and Related Stars*, ed. M. Breger & M. Montgomery, 3
- Breger, M., & Montgomery, M. H. 2014, *ApJ*, 783, 89, doi: [10.1088/0004-637X/783/2/89](https://doi.org/10.1088/0004-637X/783/2/89)
- Breger, M., & Pamyatnykh, A. A. 1998, *Astronomy and Astrophysics*, 332, 958, <https://arxiv.org/abs/astro-ph/9802076>
- Breger, M., Fossati, L., Balona, L., et al. 2012, *ApJ*, 759, 62, doi: [10.1088/0004-637X/759/1/62](https://doi.org/10.1088/0004-637X/759/1/62)
- Buchler, J. R., Goupil, M. J., & Hansen, C. J. 1997, *Astronomy and Astrophysics*, 321, 159
- Catelan, M., & Smith, H. A. 2015, *Pulsating Stars*

- Duguid, C. D., Barker, A. J., & Jones, C. A. 2020, MNRAS, 497, 3400, doi: [10.1093/mnras/staa2216](https://doi.org/10.1093/mnras/staa2216)
- Dziembowski, W. 1982, Acta Astronomica, 32, 147
- Dziembowski, W., & Krolikowska, M. 1985, Acta Astronomica, 35, 5
- Dziembowski, W., Krolikowska, M., & Kosovichev, A. 1988, Acta Astronomica, 38, 61
- Goldstein, J., & Townsend, R. H. D. 2020, The Astrophysical Journal, 899, 116, doi: [10.3847/1538-4357/aba748](https://doi.org/10.3847/1538-4357/aba748)
- Goupil, M. J., Dupret, M. A., Samadi, R., et al. 2005, Journal of Astrophysics and Astronomy, 26, 249, doi: [10.1007/BF02702333](https://doi.org/10.1007/BF02702333)
- Guzik, J. A. 2021, Frontiers in Astronomy and Space Sciences, 8, 55, doi: [10.3389/fspas.2021.653558](https://doi.org/10.3389/fspas.2021.653558)
- Higgins, T. P., & Kopal, Z. 1968, Astrophysics and Space Science, 2, 352, doi: [10.1007/BF00650913](https://doi.org/10.1007/BF00650913)
- Lai, D. 1994, Monthly Notices of the Royal Astronomical Society, 270, 611, doi: [10.1093/mnras/270.3.611](https://doi.org/10.1093/mnras/270.3.611)
- Moskalik, P. 1985, Acta Astronomica, 35, 229
- Moskalik, P., & Buchler, J. R. 1990, The Astrophysical Journal, 355, 590, doi: [10.1086/168792](https://doi.org/10.1086/168792)
- Nowakowski, R. M. 2005, Acta Astronomica, 55, 1. <https://arxiv.org/abs/astro-ph/0501510>
- Paxton, B., Smolec, R., Schwab, J., et al. 2019, ApJS, 243, 10, doi: [10.3847/1538-4365/ab2241](https://doi.org/10.3847/1538-4365/ab2241)
- Rodríguez, E., & Breger, M. 2001, A&A, 366, 178, doi: [10.1051/0004-6361:20000205](https://doi.org/10.1051/0004-6361:20000205)
- Rodríguez, E., López de Coca, P., Costa, V., & Martín, S. 1995, Astronomy and Astrophysics, 299, 108
- Schenk, A. K., Arras, P., Flanagan, É. É., Teukolsky, S. A., & Wasserman, I. 2001, PhRvD, 65, 024001, doi: [10.1103/PhysRevD.65.024001](https://doi.org/10.1103/PhysRevD.65.024001)
- Townsend, R. H. D., Goldstein, J., & Zweibel, E. G. 2018, Monthly Notices of the Royal Astronomical Society, 475, 879, doi: [10.1093/mnras/stx3142](https://doi.org/10.1093/mnras/stx3142)
- Townsend, R. H. D., & Teitler, S. A. 2013, MNRAS, 435, 3406, doi: [10.1093/mnras/stt1533](https://doi.org/10.1093/mnras/stt1533)
- Uytterhoeven, K., Moya, A., Grigahcène, A., et al. 2011, Astronomy and Astrophysics, 534, A125, doi: [10.1051/0004-6361/201117368](https://doi.org/10.1051/0004-6361/201117368)
- Weinberg, N. N., & Arras, P. 2019, The Astrophysical Journal, 873, 67, doi: [10.3847/1538-4357/ab0204](https://doi.org/10.3847/1538-4357/ab0204)
- Weinberg, N. N., Arras, P., & Pramanik, D. 2021, The Astrophysical Journal, 918, 70, doi: [10.3847/1538-4357/ac0fdd](https://doi.org/10.3847/1538-4357/ac0fdd)
- Weinberg, N. N., Arras, P., Quataert, E., & Burkart, J. 2012, ApJ, 751, 136, doi: [10.1088/0004-637X/751/2/136](https://doi.org/10.1088/0004-637X/751/2/136)